Mater. Res. Soc. Symp. Proc. Vol. 1182 © 2009 Materials Research Society 1182-EE13-42

An Integral Equation based Numerical Solution for Nanoparticles Illuminated with Collimated and Focused Light

Kursat Sendur
Sabanci University, Istanbul, 34956, Turkey.

ABSTRACT

An integral equation based numerical solution is developed when the particles are illuminated with collimated and focused incident beams. The solution procedure uses the method of weighted residuals, in which the integral equation is reduced to a matrix equation and then solved for the unknown electric field distribution. In the solution procedure, the effects of the surrounding medium and boundaries are taken into account using a Green's function formulation. Therefore, there is no additional error due to artificial boundary conditions unlike differential equation based techniques, such as finite difference time domain and finite element method. In this formulation, only the scattering nano-particle is discretized. The results are compared to the analytical Mie series solution for spherical particles, as well as to the finite element method for rectangular metallic particles. The Richards-Wolf vector field equations are combined with the integral equation based formulation to model the interaction of nanoparticles with linearly and radially polarized incident focused beams.

INTRODUCTION

Nano-optics is a rapidly growing field with a diverse set of existing and emerging practical applications [1-5]. A number of parameters have to be optimized in order to achieve large transmission efficiency while keeping the optical spot size well below the diffraction limit. Selecting an optimum set of parameters for a nano-optical transducer is important in achieving small spots and large transmission efficiencies. Due to the large number of geometry, material composition, and source-related parameters in nano-optical systems, the simulation times can be too large to optimize practical nano-optical systems.

To obtain accurate and fast computational solutions of nano-optical systems that involve a large number of geometry, material composition, and source-related parameters, the development of efficient and accurate modeling and simulation tools for near-field optical systems is necessary. In this study, an integral equation based numerical solution is developed for nano-optical particles when they are illuminated with collimated and focused incident beams. The numerical technique developed in this study requires only the discretization of the nano-optical transducer, rather than the entire structure. Therefore, it results in a fewer number of unknowns than the numerical algorithms currently being utilized for solutions of nano-optical systems, such as finite difference time domain and finite element method.

In this work, we provide a formulation for an integral equation based modeling and design tool for nano-optical systems. Similar tools have been successfully used for the analysis and design of other nano-optical systems in the literature. Nano-optical system modeling studies in the literature utilize differential equation based approaches, such as finite difference time domain (FDTD) [6-11] and finite element method (FEM) [11,12], as well as integral equation based techniques [13-20]. Previous integral equation based techniques have not presented three-dimensional results when the incidence excitation is composed of linearly and radially polarized

tightly focused beams. A tightly focused beam of incident light provides a large incident electric field onto nanoparticles, improving the near-field radiation in the vicinity of the particle. Therefore, it is desirable to obtain integral equation based solutions when the incidence excitation is composed of linearly and radially polarized tightly focused beams. In this study, a three-dimensional integral equation based solution is obtained when the incidence excitation is composed of linearly and radially polarized tightly focused beams.

A full-wave implementation of the method of weighted residuals (MWR) [21-25], which is also known as the method of moments (MoM), has a number of advantages over FDTD and FEM for nano-optical system analysis. In MWR, the effects of the surrounding medium and boundaries are taken into account using a Green's function formulation. Therefore, MWR requires only the discretization of the nano-optical transducer, whereas FDTD and FEM require the discretization of the entire computational space. Therefore, the resulting matrix equations of the MWR are smaller in size. An additional advantage of an integral equation based approach is the reduction of the additional error due to the discretization of the boundaries. In an integral equation based approach, the boundary conditions are handled in Green's function formulation; therefore, there is no additional error due to the discretization of the boundaries. In a differential equation based approach, such as FDTD and FEM, however, there is additional error introduced into the solution due to artificial boundary conditions. In addition, the integration of complicated excitation functions, such as focused beams in a dense medium, is easier in an integral equation based MWR compared to FDTD.

In this work we provide a formulation of the integral equation based numerical solution. The integral equation is discretized into a matrix equation using the method of weighted residuals. In this study, the results of the numerical technique are compared to the results of the analytical Mie series solution for spherical particles and the finite element method for rectangular metallic particles. We also extended the formulation to the case where the incident excitation is defined as a focused beam of light. Richards-Wolf vector field equations are combined with the integral equation based formulation to model linearly and radially polarized focused beams.

METHOD OF WEIGHTED RESIDUALS

The total electric field is a result of the interaction of an incident optical beam with a nanoparticle. The total electric field $\vec{E}_{tot}(\vec{r})$ is composed of two components

$$\vec{E}_{tot}(\vec{r}) = \vec{E}_{inc}(\vec{r}) + \vec{E}_{scat}(\vec{r}) \tag{1}$$

where $\vec{E}_{inc}(\vec{r})$ and $\vec{E}_{scat}(\vec{r})$ are the incident and scattered electric field components, respectively. The incident electric field can be defined as the electric field propagating in space in the absence of a scattering object. The scattered electric field $\vec{E}_{scat}(\vec{r})$ in Eq. (1) represents the fields resulting from the interaction of the incident field $\vec{E}_{inc}(\vec{r})$ with the particles. In three-dimensional space, the scattered field $\vec{E}_{scat}(\vec{r})$ can be written as

$$\vec{E}_{scat}(\vec{r}) = \frac{i\omega\mu}{4\pi}\iint_{S'} dS' \overline{\overline{G}}(\vec{r},\vec{r}') \cdot \vec{J}(\vec{r}') \tag{2}$$

where $\vec{J}(\vec{r})$ is the induced current over the particle, ω is the angular frequency, μ is the permeability, and

$$\overline{\overline{G}}(\vec{r},\vec{r}') = \left[\overline{\overline{I}} + \frac{\nabla\nabla}{k^2}\right]\frac{e^{ik|\vec{r}-\vec{r}'|}}{|\vec{r}-\vec{r}'|} \tag{3}$$

is the dyadic Green's function in free space . To solve $\vec{J}(\vec{r})$, we will expand it into a summation

$$\vec{J}(\vec{r}) \cong \sum_{j=1}^{N} I_j \vec{b}_j(\vec{r}) \tag{4}$$

where $\vec{b}_j(\vec{r})$ represents known basis functions with unknown coefficients I_j. In this work, triangular rooftop basis functions are used to discretize the induced current over the nanoparticle. These basis functions are originally proposed by Glisson and Wilton [26] on rectangular domains and used on triangular domains by Rao et al. [27]. Triangular rooftop basis functions have been very popular due to their ability to model realistic geometries. Particle geometry is discretized in order to expand the induced current with triangular basis functions.

By utilizing the expansion given in Eq. (4), the electric field integral equation is obtained as

$$-\vec{E}_{inc}^{tng}(\vec{r}) \cong \sum_{j=1}^{N} I_j \left\{ \hat{t} \cdot \frac{i\omega\mu}{4\pi} \iint_{S'} dS' \left[\overline{\overline{I}} + \frac{\nabla\nabla}{k^2}\right]\frac{e^{ik|\vec{r}-\vec{r}'|}}{|\vec{r}-\vec{r}'|} \cdot \vec{b}_j(\vec{r}') \right\} \tag{5}$$

Due to the approximation of the induced current with the summation in Eq. (4), there is a residual error in Eq. (5). The residual error in space can be written as

$$\vec{\Re}(\vec{r}) = \vec{E}_{inc}^{tng}(\vec{r}) + \sum_{j=1}^{N} I_j \left\{ \hat{t} \cdot \frac{i\omega\mu}{4\pi} \iint_{S'} dS' \left[\overline{\overline{I}} + \frac{\nabla\nabla}{k^2}\right]\frac{e^{ik|\vec{r}-\vec{r}'|}}{|\vec{r}-\vec{r}'|} \cdot \vec{b}_j(\vec{r}') \right\} \tag{6}$$

In the method of weighted residuals the error is distributed so that it is minimized in the minimum mean square sense. For this purpose, a new set of functions, known as weighting functions $\vec{w}_i(\vec{r})$ are used. The residual error $\Re(\vec{r})$ is distributed in space by equating the inner product of the residual error $\Re(\vec{r})$ with the weighting function $\vec{w}_i(\vec{r})$ to zero

$$\left\langle \vec{\Re}(\vec{r}), \vec{\omega}_i(\vec{r}) \right\rangle = \int_{\Omega} \vec{\Re}(\vec{r}) \cdot \vec{\omega}_i(\vec{r}) d\vec{r} = 0 \tag{7}$$

By placing the weighting functions into Eq. (7) we can obtain the resulting equations for the unknown coefficients of the basis functions. After mathematical manipulations, the result can be expressed as a system of linear equations as

$$\overline{\overline{Z}} \cdot \overline{I} = \overline{V} \tag{8}$$

where $Z_{i,j}$ is the impedance matrix element on the ith row and jth column which is given as

$$Z_{i,j} = \frac{i\omega\mu}{4\pi}\left[\iint_S dS \vec{w}_i(\vec{r}) \cdot \iint_{S'} dS' \frac{e^{ik|\vec{r}-\vec{r}'|}}{|\vec{r}-\vec{r}'|}\vec{b}_j(\vec{r}') + \iint_S dS \vec{w}_i(\vec{r}) \cdot \frac{\nabla\nabla}{k^2} \cdot \iint_{S'} dS' \frac{e^{ik|\vec{r}-\vec{r}'|}}{|\vec{r}-\vec{r}'|}\vec{b}_j(\vec{r}') \right] \tag{9}$$

and V_i is the excitation source element on the ith row given as

$$V_i = -\iint_S dS \vec{w}_i(\vec{r}) \cdot \vec{E}_{inc}(\vec{r}) \tag{10}$$

By solving the matrix equation in Eq. (8), we obtain the unknown coefficients of the basis functions in the induced current expansion in Eq. (4).

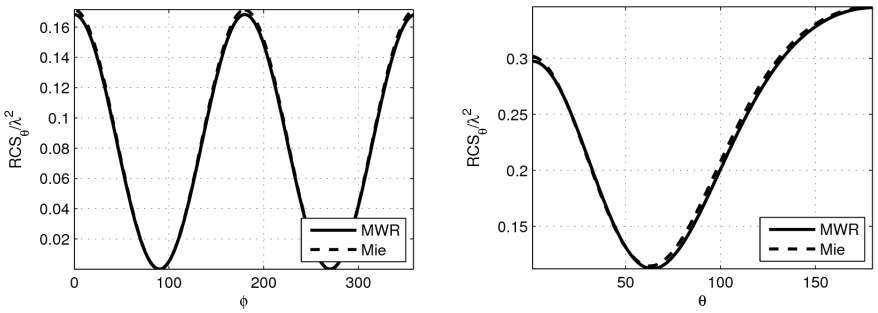

(a) (b)

Figure 1. A comparison of the MWR results with the Mie series solution for the RCS of a conducting sphere with a radius of 140 nm. The operating wavelength is 700 nm. θ and ϕ components of the radar cross section are plotted on various cuts: (a) RCS_θ as a function of ϕ on θ=90° cut, (b) RCS_θ as a function of θ on ϕ=0° cut.

Using the integral equation based formulation given in the previous section, the interactions of a collimated beam with both a conducting metallic sphere and cube are studied. The collimated beam is modeled as a linearly polarized plane wave propagating in the z direction. In Fig. 1, the radar cross section of a sphere with a radius of 140 nm is presented to compare MWR results with the analytical Mie series solution. The operating wavelength of the laser source is 700 nm. A comparison of the MWR results with the analytical Mie series solution shows a good agreement between the results.

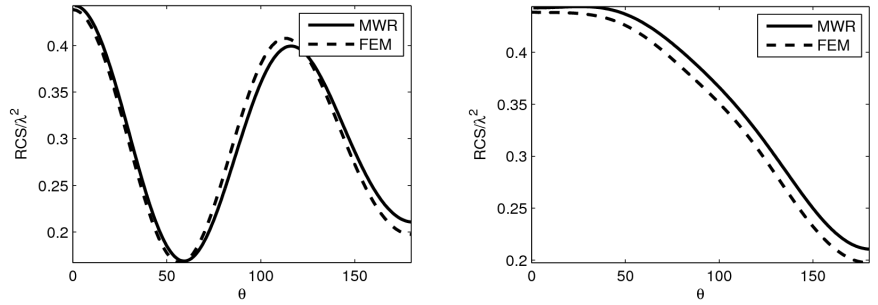

(a) (b)

Figure 2. A comparison of the FEM and MWR results for the radar cross section of a conducting cube with a side length of 200 nm. The operating wavelength for the incident beam is 700 nm. θ component of the radar cross section is plotted on various ϕ cuts: (a) RCS_θ as a function of θ on ϕ=0° cut, (b) RCS_θ as a function of θ on ϕ=90° cut.

In Fig. 2, the scattering cross section of a conducting metallic cube with a side length of 200 nm is obtained on various cuts in the far-field. There is no analytical solution for a cube, therefore, we utilized an FEM solution as a reference. Similar to the previous calculations, a linearly polarized plane wave is utilized. The operating wavelength is 700 nm. In Fig. 2 (a) and (b) the θ component of the radar cross section is plotted on ϕ=0° and ϕ=90° cuts. The MWR and FEM results show a good agreement.

LINEARLY AND RADIALLY POLARIZED FOCUSED BEAMS

It is also very desirable to obtain solutions when the incidence excitation is composed of linearly and radially polarized focused beams. In the previous section, the integral equation

based solutions are provided when the incident beam is a plane wave. In this section, the solution is obtained for the case where the incident beam is a focused beam. Richards and Wolf developed a method for calculating the electric field semi-analytically near the focus of an aplanatic lens [28, 29]. Using the Richards-Wolf method, we can obtain both transverse and longitudinal components near the focus for both linear and radial polarizations.

In Fig. 3 (a), various components of the near-field radiation from a sphere are plotted when the incident beam is a linearly polarized focused beam obtained from an optical lens system with a numerical aperture of 0.85. The operating frequency is 700 nm. The results are plotted for spherical particles with radii 70 and 140 nm. The E_x and E_z components are plotted on the $\phi = \pi/2$ cut as a function of θ. For small spheres, the E_x component has a maximum at $\theta = \pi/2$. As the spherical particle gets larger, we observe a shift of the location at which the E_x component has a maximum field. This is due to the increased interaction between a larger sphere and a wider range of angular components of a focused beam. As the size of the spherical particle gets larger, the particle interacts more with components that are incident to larger angles. A similar shift is also observed in the E_z component, as shown in Fig. 3 (a).

In Fig. 3 (b), various components of the near-field electric field are plotted for a radially polarized incidence beam. The results are plotted for spherical particles with radii 70 and 140 nm. E_x and E_z components are plotted on the $\phi = \pi/2$ cut as a function of θ. The incident beam parameters are identical to the previous set of results with the exception that a radial polarization is used instead of a linear polarization. Contrary to the results in Fig. 3 (a), E_x shows a minimum at $\theta = \pi/2$ in Fig. 3 (b). This is due to the difference in the strength of various components of the linearly and radially polarized incident focused beams. For the linearly polarized focused wave, the *x*-component of the electric field is much stronger than the other two components. The radially polarized wave, on the other hand, has a strong *z*-component in the focal region.

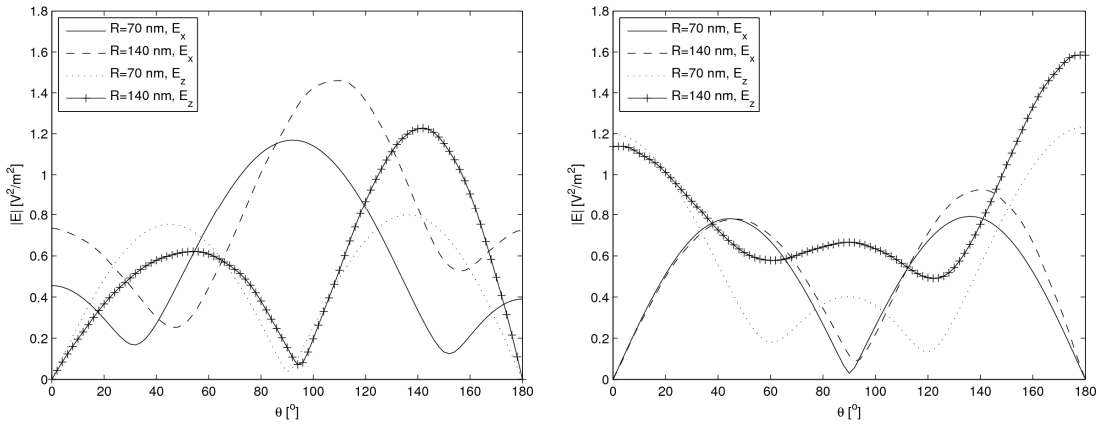

Figure 3. Electric field components when a focused beam of light interacts with spheres of various sizes: (a) linearly polarization, (b) radial polarization.

CONCLUSIONS

In summary, an integral equation based numerical solution was developed. The formulations for both plane waves and focused beams were given. For focused beams, the Richards-Wolf vector field equations were combined with the integral equation based

formulation to model both linearly and radially polarized focused beams. The results of the integral equation based solution were compared to the results of the analytical Mie series solution for spherical particles and the finite element method for rectangular metallic particles. The methods showed a good agreement.

REFERENCES

1. T. D. Milster, "Horizons for optical data storage," Optics and Photonics News **16**, 28–32 (2005).
2. R. E. Rottmayer, S. Batra, D. Buechel, W. A. Challener, J. Hohlfeld, Y. Kubota, L. Li, B. Lu, C. Mihalcea, K. Mountfield, K. Pelhos, C. Peng, T. Rausch, M. A. Seigler, D. Weller, and X. Yang, IEEE Trans. Magn. **42**, 2417–2421 (2006).
3. A. Hartschuh, E. J. Sanchez, X. S. Xie, and L. Novonty, Phys. Rev. Lett. **90**, 095503 (2003).
4. L. Wang and X. Xu, J. Microsc. **229**, 483–489 (2008).
5. B. Liedberg, C. Nylander, I. Lundstroem, Sens. Actuators **4**, 299–304 (1983).
6. W. A. Challener, I. K. Sendur, and C. Peng, Opt. Express **11**, 3160–3170 (2003).
7. J. T. II Krug, E. J. Sánchez, and X. S. Xie, J. Chem. Phys. **116,** 10895 (2002).
8. T. Yamaguchi, Electron. Lett. **44,** 4455427 (2008).
9. T. Yamaguchi and T. Hinata, Opt. Express **15**, 11481-11491 (2007).
10. L. Liu and S. He, Appl. Opt. **44**, 3429-3437 (2005).
11. T. Grosges, A. Vial, and D. Barchiesi, Opt. Express **13**, 8483-8497 (2005).
12. K. Sendur, W. Challener, and C. Peng, J. Appl. Phys. **96**, 2743–2752 (2004).
13. J. P. Kottmann and O. J. F. Martin, Opt. Express **8**, 655-663 (2001).
14. J. P. Kottmann and O. J. F. Martin, IEEE Trans. Antennas Propag. **48**, 1719-1726 (2000).
15. J. P. Kottmann, O. J. F. Martin, D. R. Smith, and S. Schultz, Chem. Phys. Lett. **341**, 1-6 (2001).
16. J. P. Kottmann, O. J. F. Martin, D. R. Smith, and S. Schultz, New J. Phys. **2**, 27 (2000).
17. J. Jung and T. Sondergaard, Phys. Rev. B **77**, 245310 (2008).
18. F. J. Garcia de Abajo and A. Howie, Phys. Rev. B **65**, 115418 (2002).
19. V. Myroshnychenko et al., Adv. Mater. **20**, 4288-4293 (2008).
20. V. Myroshnychenko et al., Chem. Soc. Rev. **37**, 1792-1805 (2008).
21. J. H. Richmond, Proc. IEEE **53**, 796-804 (1965).
22. R. F. Harrington, Proc. IEEE **55**, 136-149 (1967).
23. R. F. Harrington, *Field Computation by Moment Methods*, (IEEE Press, New York, NY, 1993).
24. E. K. Miller, L. Medgyesi-Mitschang, and E. H. Newman, Eds., *Computational Electromagnetics* (IEEE Press, New York, NY, 1992).
25. R. C. Hansen, Ed., *Moment Methods in Antennas and Scattering*, (Artech, Boston, MA, 1990).
26. A. W. Glisson and D. R. Wilton, IEEE Trans. Antennas Propag. **28**, 593-603 (1982).
27. S. M. Rao, D. R. Wilton, and A. W. Glisson, IEEE Trans. Antennas Propag. **30**, 409-418 (1982).
28. E. Wolf, Philos. Trans. R. Soc. London Ser. A **253**, 349-357 (1959).
29. B. Richards and E. Wolf, Philos. Trans. R. Soc. London Ser. A **253**, 358-379 (1959).